Environmental Science & Technology

pubs.acs.org/est

Article

Impacts of Chemical Degradation on the Global Budget of Atmospheric Levoglucosan and Its Use As a Biomass Burning Tracer

Yumin Li, Tzung-May Fu,* Jian Zhen Yu,* Xu Feng, Lijuan Zhang, Jing Chen, Suresh Kumar Reddy Boreddy, Kimitaka Kawamura, Pingqing Fu, Xin Yang, Lei Zhu, and Zhenzhong Zeng

Cite This: https://doi.org/10.1021/acs.est.0c07313

Read Online

ACCESS | Metrics & More | Article Recommendations | Supporting Information

ABSTRACT: Levoglucosan has been widely used to quantitatively assess biomass burning's contribution to ambient aerosols, but previous such assessments have not accounted for levoglucosan's degradation in the atmosphere. We develop the first global simulation of atmospheric levoglucosan, explicitly accounting for its chemical degradation, to evaluate the impacts on levoglucosan's use in quantitative aerosol source apportionment. Levoglucosan is emitted into the atmosphere from the burning of plant matter in open fires (1.7 Tg yr^{-1}) and as biofuels (2.1 Tg yr^{-1}). Sinks of atmospheric levoglucosan include aqueous-phase oxidation (2.9 Tg yr^{-1}), heterogeneous oxidation (0.16 Tg yr^{-1}), gas-phase oxidation (1.4×10^{-4} Tg yr^{-1}), and dry and wet deposition (0.27 and 0.43 Tg yr^{-1}). The global atmospheric burden of levoglucosan is 19 Gg with a lifetime of 1.8 days. Observations show a sharp decline in levoglucosan's concentrations and its relative abundance to organic carbon aerosol (OC) and particulate K^+ from near-source to remote sites. We show that such features can only be reproduced when levoglucosan's chemical degradation is included in the model. Using model results, we develop statistical parametrizations to account for the atmospheric degradation in levoglucosan measurements, improving their use for quantitative aerosol source apportionment.

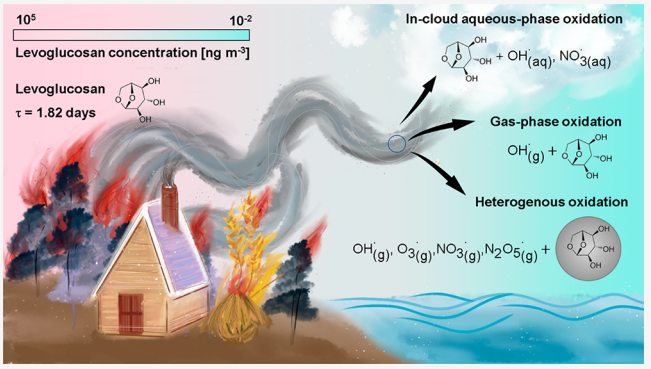

KEYWORDS: *levoglucosan, biomass burning, atmospheric degradation, aqueous-phase oxidation, heterogeneous reaction, source apportionment*

1. INTRODUCTION

Levoglucosan (1,6-anhydro-β-D-glucopyranose), a water-soluble anhydrosugar produced by the thermal breakdown of cellulose, has been widely used as a molecular tracer for biomass burning.[1,2] Biomass burning, defined here as the burning of plant matter in open fires and as biofuels, is a large source of aerosols in the troposphere, affecting air quality and climate on regional and global scales.[3−5] It is thus vital to quantify the contributions of biomass burning to ambient aerosols, to understand its impacts and inform emission reduction efforts. Many studies have used the measured abundance of levoglucosan relative to organic carbon aerosols (OC) to estimate the contribution of biomass burning to the ambient OC at a receptor site (eq 1):

$$\text{contribution of biomass burning to OC}(\%) = \frac{\left(\frac{[L]}{[OC]}\right)_{\text{ambient}}}{ER_{\text{levoglucosan,OC}}} \times 100\% \quad (1)$$

where $([L]/[OC])_{ambient}$ is the abundance of levoglucosan relative to OC measured in an ambient air mass. $ER_{levoglucosan,OC}$ is the emission ratio of the two constituents from the biomass burning source.[6−9] For example, using eq 1 the annual mean contribution of biomass burning to ambient OC was estimated to be 33% in Guangdong, China, reflecting the local use of crop residues as a residential energy source.[7]

The use of eq 1 assumes that, during the transport of the sampled air mass from the biomass burning area to the receptor site, the concentration ratio of levoglucosan to OC associated with that biomass burning source is equal to $ER_{levoglucosan,OC}$ of that source and does not change. However, there are few reported values of $ER_{levoglucosan,OC}$, and they vary greatly by fuel types and combustion conditions.[6−9] Also, gaseous precursors emitted from the biomass burning source

Received: October 29, 2020
Revised: March 8, 2021
Accepted: March 9, 2021

may produce secondary OC during transport.[10] Most importantly, laboratory experiments and field measurements have shown that atmospheric levoglucosan is chemically reactive,[1,11−17] resulting in its faster removal from the atmosphere relative to OC.[15,18] Previous studies have not considered the chemical degradation of levoglucosan when using eq 1 for aerosol source apportionment and likely underestimated the contributions of biomass burning at receptor sites.

Laboratory experiments showed that levoglucosan can be oxidized in the gas[16] and aqueous phases[1,11,17] or be heterogeneously oxidized on aerosol surfaces.[12−14,19,20] Significant degradation of atmospheric levoglucosan has also been observed in the field.[15,18,21] Levoglucosan is semivolatile; after its pyrogenic production, it mostly condenses onto fine particles with only 6−20% in the gas phase.[1,22] The atmospheric lifetime of levoglucosan against gas-phase oxidation (defined as the burden of levoglucosan divided by the loss rate due to gas-phase oxidation) is estimated to be 26 days under typical atmospheric OH levels ($[OH]_g = 2.0 \times 10^6$ molecules cm^{-3}).[16] In comparison, the aqueous-phase and heterogeneous removal of levoglucosan from the atmosphere are likely much faster. The measured residence time of levoglucosan in an aqueous solution with $[OH]_{aq} = 3 \times 10^{-13}$ M (high-end of typical in-cloud concentrations)[23,24] is 6−23 min,[11] which extrapolates to an atmospheric lifetime of levoglucosan against aqueous oxidation of 0.5−4 days.[11] The estimated atmospheric lifetimes of particulate levoglucosan against heterogeneous oxidation are 5.8 min by O_3-oxidation,[13] 112 min by NO_3-oxidation,[13] 30 min by N_2O_5,[13] and 0.7 to 53 days by OH,[12,14,19,20,25,26] under polluted conditions. A recent box model simulation estimated the levoglucosan's atmospheric lifetimes against gas-phase and heterogeneous removal to range between 8 h and 10 days.[27] These estimated atmospheric lifetimes of levoglucosan against chemical removal are comparable to the lifetimes of fine, soluble particulates against dry and wet deposition.[1] Therefore, chemical degradation must be considered when interpreting the atmospheric concentrations of levoglucosan.

Here, we construct the first global simulation of atmospheric levoglucosan, accounting for its emissions from biomass burning, its chemical removal, and dry and wet deposition. We compare simulation results against global observations to assess the impacts of chemical degradation on the observed concentrations of levoglucosan and its relative abundances to OC and particulate K^+ (both emitted in large amounts from biomass burning) at near-source and remote sites. Particulate K^+ is not known to chemically degrade in the atmosphere; therefore, the concentration ratios of levoglucosan to particulate K^+ highlight the effects of levoglucosan's degradation. Finally, we use model results to statistically correct for the atmospheric degradation of levoglucosan in eq 1, improving the quantitative assessment of biomass burning's contribution to ambient OC.

2. MODEL AND DATA

2.1. GEOS-Chem Model. We modify the GEOS-Chem global 3-D chemical transport model (v12.3.0, http://geos-chem.org)[28] to simulate levoglucosan, OC, K^+ in fine particulate matter ($PM_{2.5}$) and gas-phase levoglucosan for the year 2013, to evaluate the impacts of levoglucosan's degradation. Our GEOS-Chem simulation is driven by the GEOS-FP assimilated meteorological data set (https://gmao.gsfc.nasa.gov/GMAO_products/) at 5° longitude ×4° latitude resolution with 72 vertical layers. GEOS-Chem includes a comprehensive tropospheric HO_x-NO_x-VOC-ozone-halogen-aerosol chemical mechanism.[29−31] Aerosols in the standard GEOS-Chem include dust, sea salt, elemental carbon aerosol, primary OC, sulfate, nitrate, ammonium, and secondary organic aerosol (SOA).[32−35] Freshly emitted OC is assumed to be 50% hydrophobic and 50% hydrophilic, with a conversion time scale from hydrophobic to hydrophilic of 1.2 days.[32] SOA is produced at irreversible yields from anthropogenic, biomass burning, and biogenic precursors.[35] Dry deposition of aerosols and gases are simulated by a resistance-in-series scheme.[36,37] Wet deposition of aerosols and gases include rain−out and wash-out;[38,39] the wash-out efficiency for hydrophilic fine particles is assumed to be unity.

Global monthly anthropogenic emissions for OC (except from biofuel burning) and other pollutants are from the Community Emissions Data System[40] (CEDS) but superseded by improved inventories in regions where better information is available (Supporting Information (SI) Text S1). Further details of the GEOS-Chem model and the emission inventories for other pollutants are given in SI Text S1. We spin-up the model throughout the year 2013 and use the result to restart the simulation on January 1, 2013.

2.2. Emissions of Levoglucosan, OC, and Particulate K^+ from Biomass Burning. Biomass burning is the dominant source of levoglucosan and a major source of OC and K^+ in the atmosphere.[1,2,5,41,42] Recent studies showed that there are anthropogenic, non-biomass burning emissions (e.g., municipal waste incineration) of levoglucosan, but those emissions are minor and likely still related to the pyrolysis of cellulose.[42,43] We use monthly estimates of dry vegetative mass burned in open fires from the Global Fire Emissions Database[4] (GFEDv4.1s) inventory[4] for the year 2013. GFED v4.1s estimate burned dry biomass base on the Carnegie-Ames-Standard Approach biogeochemistry model[44] and the land cover and burned area products from MODIS. Burned areas associated with small fires (e.g., crop residue burning) are statistically estimated using MODIS observations.[4,45] The estimated global dry biomass burned in open fires is 3638 Tg for the year 2013, mostly of savanna and grassland (59%) and forest (23%) burning.

For OC emissions from solid biofuel burning in the year 2013, we use the monthly emission estimates from CEDS[40] over most of the world, superseded by the annual emission estimates from the Diffuse and Inefficient Combustion Emissions in Africa inventory (DICE-Africa)[46] over Africa. CEDS estimates OC emissions from solid biofuel use in three sectors: (1) energy generation, (2) industrial combustion and processes, and (3) residential, commercial, and other sources. Activity rates and emission factors for energy generation and industries are from the Speciated Pollutant Emission Wizard data set.[47] Activity rates for residential, commercial, and other sources are estimated by country and fuel type.[40] DICE-Africa[46] estimates OC emissions from the use of four solid biofuels (household fuelwood, commercial fuelwood, crop residue, and charcoal), as well as OC emissions from charcoal production. Activity rates are from country-level energy statistics.[48] The emission factors for OC in DICE-Africa are fuel-specific and vary by combustion efficiency (flaming or smoldering). Overall, the estimated global annual OC emission from biofuel use for 2013 is 9.2 Tg C, 82% of which is from residential and commercial activities.

https://doi.org/10.1021/acs.est.0c07313
Environ. Sci. Technol. XXXX, XXX, XXX−XXX

Table 1. Summary of Emission Factors and Emission Ratios from Biomass Burning Used in This Study[a]

types of biomass	emission factors (g per kg dry matter)			emission ratios (g g^{-1})	
	levoglucosan	K^+	OC	$ER_{levoglucosan,OC}$	$ER_{K^+,OC}$
savanna and grassland	0.20[b] (0.020−0.41)	0.42 (0.12−0.68)	3.0 (0.7−6.1)	[f]	[f]
tropical forest	0.52[c] (0.20−1.17)	0.34 (0.05−0.60)	4.4 (1.5−6.1)	[f]	[f]
temperate forest	1.33 (0.07−2.75)	0.17 (0.07−0.41)	10.9 (1.8−27.2)	[f]	[f]
boreal forest	1.87[d] (0.30−2.50)	0.17 (0.07−0.41)	8.2 (3.3−8.2)	[f]	[f]
agricultural residues	0.82 (0.007−1.84)	0.51 (0.13−1.47)	4.9 (1.0−13.0)	[f]	[f]
peat fires	1.42[e] (0.04−4.60)	0.004	14.2 (12.4−16.0)	[f]	[f]
biofuel use	[f]	[f]	[g]	0.225	0.042
charcoal making	[f]	[f]	[g]	0.075	0
charcoal burning	[f]	[f]	[g]	0.359	0.34

[a]All values were taken from Andreae[5] unless otherwise indicated. Values inside parentheses indicate the ranges reported in the literature.[43,49,53−59] [b]From a high-end value reported for Australian savannah Wang et al.[49] [c]From a high-end value reported for Amazonian forest Graham et al.[50] [d]From a high-end value reported for Canadian boreal forest Landis et al.[51] [e]From a high-end value reported for peatland Jayarathne et al.[52] [f]Not used to derive emissions. [g]Emissions as given by CEDS and DICE-Africa.

To estimate the biomass burning emissions of levoglucosan, OC, and K^+, we apply fuel-specific emission factors to the dry biomass burned in open fires and scale the OC emissions from biofuel use. We further assume that freshly emitted levoglucosan is 90% in the particle phase and 10% in the gas phase.[22] Table 1 summarizes the emission factors and emission ratios used in this study. For particulate OC and K^+, we use the mean fuel-specific open-fire emission factors compiled by Andreae,[5] or we moderately vary the emission factors within the reported standard deviations, such that the simulated OC and K^+ concentrations agree with near-source observations. For levoglucosan, we experiment within the range of emission factors reported in the literature,[5,43,49−59] to optimize the agreement between observed and simulated particulate levoglucosan concentrations at near-source sites. Similarly, we optimize the emission ratios of levoglucosan to OC ($ER_{levoglucosan,OC}$) and K^+ to OC ($ER_{K^+,OC}$) to estimate levoglucosan and K^+ emissions from biofuel, charcoal use, and charcoal production, respectively. Our optimization of levoglucosan's emission ratios from biofuel use compensate for the lack of explicit anthropogenic, nonbiomass-burning sources, which are in any case minor.[42,43]

Our model also includes particulate K^+ emissions as parts of fine dust and fine sea salt. Natural dust emissions in four size bins are from an offline inventory;[60] 100% of the first bin (0.1 to 1 μm radii) and 38% of the second bin (1−1.8 μm radii) are regarded as fine natural dust.[33,61] Fine anthropogenic dust emissions are from the Anthropogenic Fugitive, Combustion and Industrial Dust inventory.[62] We assume that particulate K^+ was 0.2% of the total fine dust mass.[63,64] Sea salt emissions in the accumulated size range (0.1−0.5 μm radii) are from Jaeglé et al.;[34] we assume 1% of that mass to be K^+.[64,65]

2.3. Atmospheric Processes of Levoglucosan.

2.3.1. The Gas/Particle Partitioning and Gas-Phase Oxidation of Levoglucosan. We partition levoglucosan between the gas and particulate phases using an equilibrium partitioning coefficient K_{OM} (m^3 μg^{-1}):[22,66]

$$K_{OM} = \frac{[L]_p}{[L]_g[M_0]} \tag{2}$$

where $[L]_p$ (ng m^{-3}) and $[L]_g$ (ng m^{-3}) are the particulate and gaseous levoglucosan concentrations, respectively. $[M_0]$ (μg m^{-3}) is the concentration of the total particulate organic matter (OM), onto which levoglucosan condenses. The K_{OM} for levoglucosan is calculated from a simple absorptive partitioning theory:[22,66]

$$K_{OM} = \frac{RT}{10^6 M_{OM} \xi_{OM} P^{vap}} \tag{3}$$

where R (m^3 atm K^{-1} mol^{-1}) is the ideal gas constant; T (K) is the air temperature; M_{OM} (200 g mol^{-1}) is the mean molecular weight of the OM substrate;[22,67] ζ_{OM} = 1 is the activity coefficient of OM.[22] $P^{vap} = P_0^{vap} \exp\left(\frac{\Delta H_{vap}}{R}\left(\frac{1}{298.15} - \frac{1}{T}\right)\right)$ (atm) is the temperature-dependent saturation vapor pressure of pure levoglucosan, with $P_0^{vap} = 2.38 \times 10^{-10}$ atm and ΔH_{vap} = 84.0 kJ mol^{-1}.[22,68,69]

Gaseous levoglucosan can be oxidized by atmospheric OH radical.[1,16] The second-order temperature-dependent reaction rate k_g (unit: cm^3 molecule^{-1} s^{-1}) is[16]

$$k_g(T) = (1.3 \pm 2.1) \times 10^{-23} T^{3.71} \exp\left(\frac{735.7}{T}\right) \tag{4}$$

2.3.2. Aqueous-Phase Oxidation of Levoglucosan. Particulate levoglucosan can be scavenged by cloud and rain, or it can dissolve in aqueous aerosols, which then activate into cloud droplets. Once in the aqueous phase, levoglucosan can be oxidized by OH and NO_3 radicals.[11,17] To the best of our knowledge, the aqueous removal of levoglucosan has thus far only been measured in bulk, dilute solutions.[11,17] A previous box model calculation using these measured aqueous reaction rates showed the lifetime of levoglucosan against aqueous oxidation in wet aerosols to be significantly longer than that in cloudwater, even at 90% relative humidity.[11] As such, in our model we only account for the aqueous oxidations of levoglucosan in clouds. The removal of levoglucosan by aqueous reactions is thus sensitive to the temperature and cloud liquid water content[11] in the atmosphere, as well as the aqueous oxidant concentrations. We use the bimolecular rate constants from Hoffmann et al.[11] to calculate the aqueous-phase oxidation rates of levoglucosan by OH (r_{OH}, in units of M s^{-1}) and NO_3 (r_{NO_3}, in units of M s^{-1}), respectively:

$$r_{OH}(T) = [L]_{aq} \cdot [OH]_{aq} \cdot (8.7 \pm 0.4) \times 10^{10} \exp\left(\frac{-1083}{T}\right) \tag{5}$$

https://doi.org/10.1021/acs.est.0c07313
Environ. Sci. Technol. XXXX, XXX, XXX−XXX

$$r_{NO_3}(T) = [L]_{aq} \cdot [NO_3]_{aq} \cdot (2.3 \pm 0.1) \times 10^{10} \exp\left(\frac{-2141}{T}\right) \quad (6)$$

$[L]_{aq}$, $[OH]_{aq}$, and $[NO_3]_{aq}$ are the in-cloud concentrations of levoglucosan, OH, and NO_3, respectively. We ignore the aqueous oxidation of levoglucosan by sulfate ion, as that reaction is 2 orders of magnitude slower than the aqueous oxidation by OH.[11]

We calculate the in-cloud concentrations of levoglucosan ($[L]_{aq}$) by assuming its scavenging efficiency by cloud (F_c). For hydrophilic particles, F_c range from near-zero for particles smaller than 0.3 μm to unity for particles larger than 1 μm.[70] We assume a constant F_c of 0.65 based on the typical observation that 80% of levoglucosan mass is in particles between 0.4 and 1 μm in size.[71,72] Cloud liquid water content in the cloudy fraction of the model grid is from GEOS-FP. The calculated in-cloud concentration of levoglucosan is always much lower than its solubility (8.23 M at 20 °C).[73]

The in-cloud concentration of NO_3 radical is calculated by the partial pressure of gaseous NO_3 (P_{NO_3}) and its Henry's law constant ($K_{NO_3} = 1.8 \cdot \exp[2000 \cdot (1/T - 1/298.15)]$, unit: M atm^{-1})[74] using eq 7. The in-cloud concentration of OH radical is calculated by eq 8 using the simulated gaseous OH concentration ($C_{OH,g}$, molecules cm^{-3}) and a simple partition coefficient $\delta = 1 \times 10^{-19}$ M cm^3 molecule^{-1}.[75] The simulated in-cloud OH concentration range from 10^{-17} to 10^{-13} M, in the lower range of the simulated values from a cloud chemistry model.[76] For remote clouds, our simulated mean in-cloud OH concentration is 10^{-16} M (range from 10^{-17} to 10^{-15} M), consistent with observed remote cloud ranges.[23]

$$[NO_3]_{aq} = K_{NO_3} P_{NO_3} \quad (7)$$

$$[OH]_{aq} = \delta \cdot C_{OH,g} \quad (8)$$

The cloud-scavenged levoglucosan mass not removed by aqueous oxidation is returned to the particulate phase upon cloud evaporation.

2.3.3. Heterogeneous Oxidation of Levoglucosan. Particulate levoglucosan can also be heterogeneously oxidized by gaseous oxidants, such as O_3, OH radical, NO_3 radical, and N_2O_5.[13] The heterogeneous oxidation of levoglucosan by a gaseous oxidant, x, is represented as a pseudo-first-order reaction,[77] where the rate constant k_x (s^{-1}) is[77]

$$k_x = \frac{1}{4} \omega_x \gamma_x A \quad (9)$$

where γ_x is the effective uptake coefficient of the oxidant x. For O_3, NO_3, and N_2O_5, we use γ_x values of $1.3(1.0-2.5) \times 10^{-5}$, $1.29(0.35-2.33) \times 10^{-3}$, and $3.7(1.0-6.4) \times 10^{-5}$, respectively, as these are the only ones available in the literature.[13] For OH, we use $\gamma_x = 0.91$, a middle-of-the-range value from the literature (0.08–27).[12,14,19,20,25,26] A is the surface area density of particulate levoglucosan (unit: m^2 m^{-3}), calculated by assuming a typical diameter of 8×10^{-7} m and a density of 1688 kg m^{-3} for levoglucosan particles. $\omega_x = 1.455 \times 10^2 \sqrt{T/MW_x \times 10^3}$ (unit: m s^{-1}) is the mean molecular velocity of x, calculated as a function of temperature and the molecular weight (MW_x, kg mol^{-1}) of the oxidant x.

2.4. Observation Data of Particulate Levoglucosan, OC, and K$^+$. SI Table S1 summarizes the published levoglucosan measurements at 56 global sites (24 urban sites, 13 rural sites, 5 forest sites, 8 marine sites, and 6 polar sites). SI Table S1 is largely based on a literature compilation by Bhattarai et al.,[41] to which we supplement with additional measurements.[21,78−80] We also compile concurrent measurements of OC and K$^+$ at 38 and 26 sites, respectively (SI Table S1). The particles sampled in each measurement vary among $PM_{2.5}$, PM_{10}, and total suspended particles (TSP). However, because 90% of the airborne particulate levoglucosan mass is in $PM_{2.5}$,[81−84] it is reasonable to combine these measurements for comparison with our model results. Many measurements in SI Table S1 sampled only during the local open-burning season, so they tended to show intense biomass burning influence. To address this issue, we sample our model results at each site during the month of the measurement when making one-on-one comparison between the measurements and the model results.

3. RESULT AND DISCUSSION

3.1. Global Emission of Levoglucosan. The global annual total levoglucosan emission is 3.8 Tg yr^{-1}, including 2.1 Tg yr^{-1} from biofuel use and 1.7 Tg yr^{-1} from open fires. Biofuel emissions (Figure 1a) are highest over Eastern China, South Asia, and the densely populated areas of Africa, reflecting the residential uses of biofuels. Biofuel emissions are relatively high over Eastern Europe, Northeastern U.S., and Eastern South America, reflecting the use of firewood use in

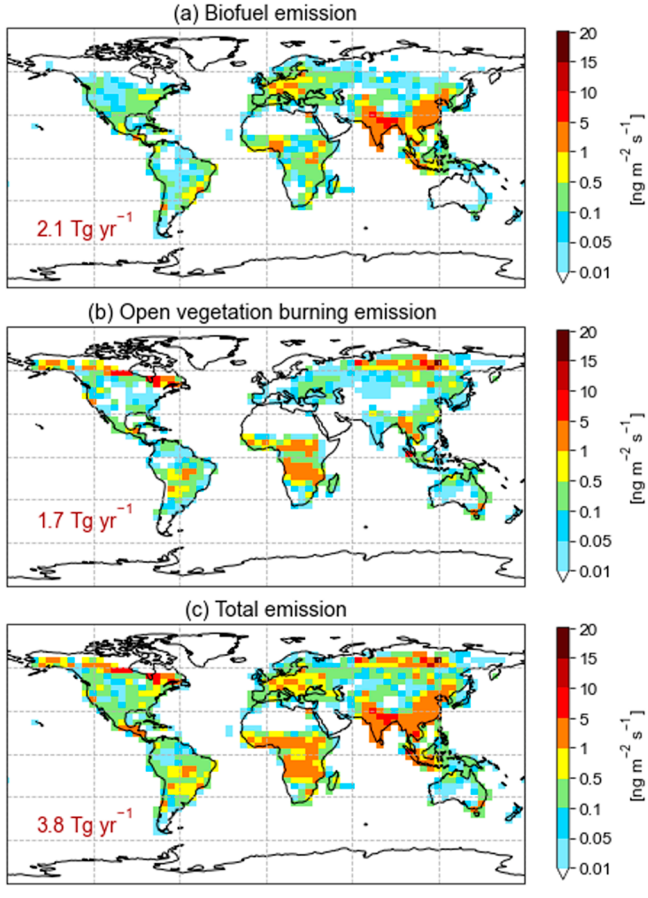

Figure 1. Annual emissions of levoglucosan (a) from total biomass burning sources, (b) from burning of plant-based solid biofuel, and (c) from burning of vegetative matter in open fires. The global annual emissions are shown inset.

https://doi.org/10.1021/acs.est.0c07313
Environ. Sci. Technol. XXXX, XXX, XXX−XXX

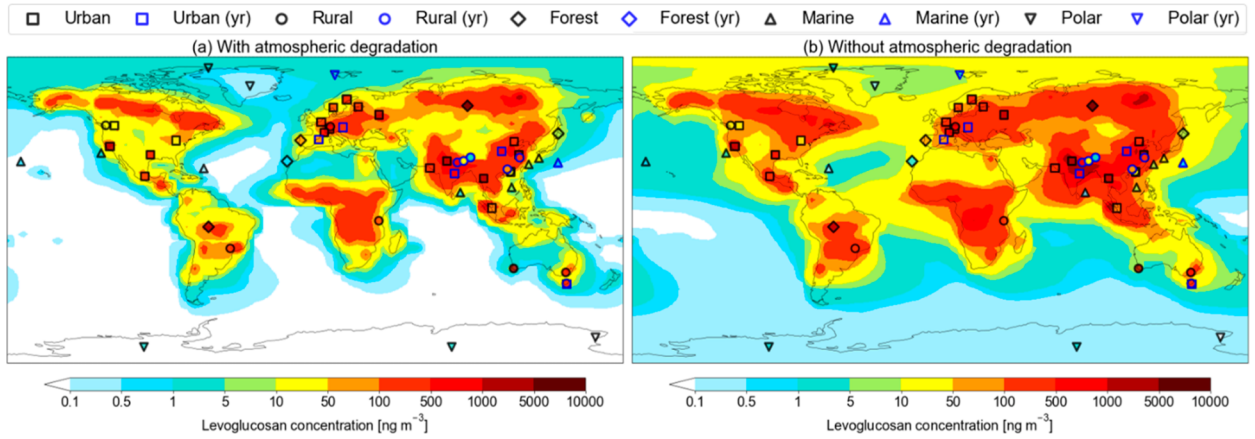

Figure 2. Simulated (filled contours) annual mean particulate levoglucosan concentrations (a) with and (b) without atmospheric degradation, compared to the observations (symbols coded by site types). Symbols with blue outlines show annual mean observations; symbols with black outlines show seasonal observations, which may be biased toward intense biomass burning influence

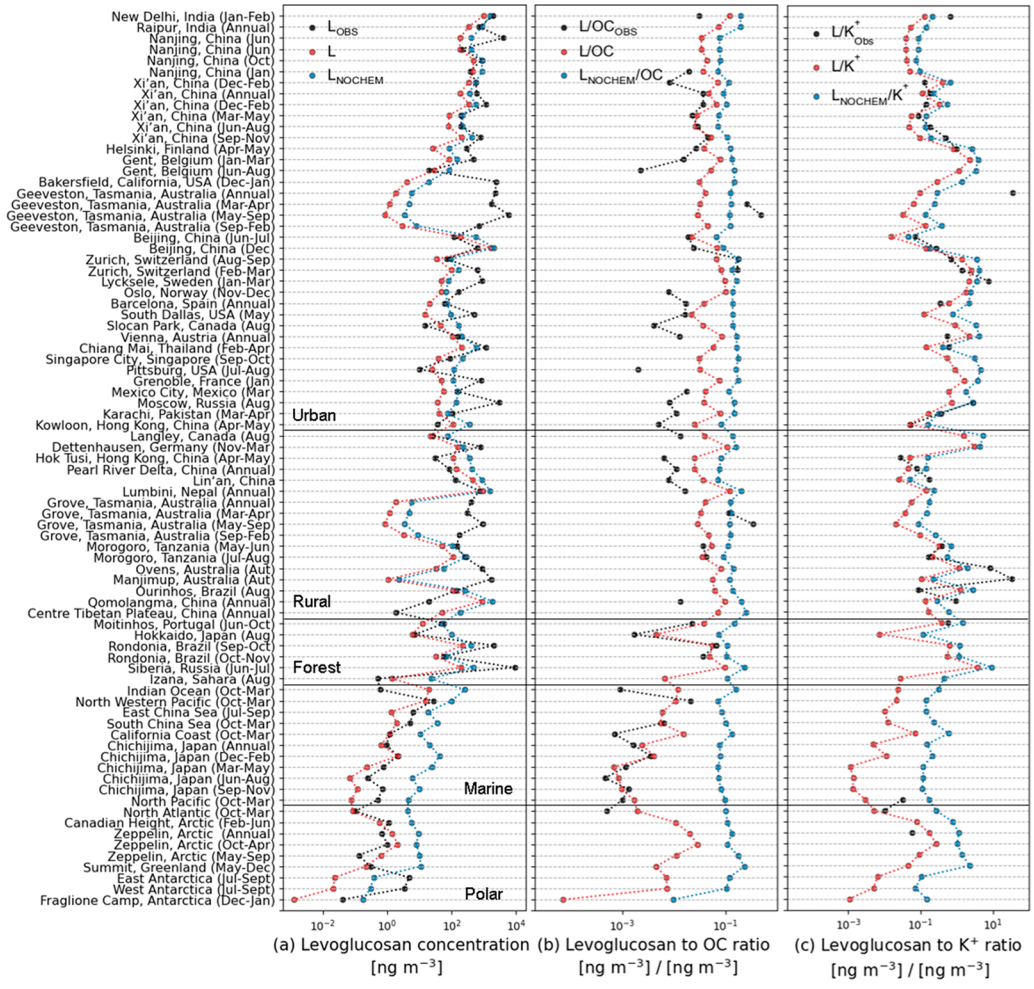

Figure 3. Comparisons of observed (black) and simulated values of (a) particulate levoglucosan concentrations, (b) particulate levoglucosan to OC concentration ratios, and (c) particulate levoglucosan to K^+ concentration ratios at global surface sites. Red and blue lines indicate simulations with and without atmospheric degradation of levoglucosan, respectively.

residential wood stoves. Open-fire emissions of levoglucosan (Figure 1b) are highest over the boreal forests of North America and Siberia, reflecting the forest fires and the high emission factors of levoglucosan from hardwoods. Open fires over the savanna and tropical forests in central Africa, as well as the open-burning of agricultural residues over Southeast Asia also emit large amounts of levoglucosan. Overall, the global levoglucosan emissions reflect the regional differences in the types and amounts of biomass burned (Figure 1c). A recent bottom-up estimate for Chinese levoglucosan emission (from biomass burning and nonbiomass burning sources) was 146 Gg for the year 2014.[42] We estimate a higher Chinese

https://doi.org/10.1021/acs.est.0c07313
Environ. Sci. Technol. XXXX, XXX, XXX−XXX

levoglucosan emission of 285 Gg for the year 2013, due to our adoption of higher emission factors/ratios, based on optimized simulation of near-source concentrations (Section 2.2).

3.2. Comparison of Observed and Simulated Concentrations of Particulate Levoglucosan and Its Relative Abundance to OC and K^+. Figure 2a shows the observed annual or seasonal particulate levoglucosan concentrations at global surface sites, which vary over 7 orders of magnitude (10^{-2} to 10^4 ng m^{-3}) with large regional differences. Observed particulate levoglucosan concentrations generally exceed 10 ng m^{-3} over populated areas and forested lands. The highest particulate levoglucosan concentration of 9220 ng m^{-3} was measured in Siberia during June-July 2012 due to a forest fire near the measurement site.[85] Observed levoglucosan concentrations are generally higher in winter than in summer at urban sites and higher in the dry season than in the wet season.[41] Outside of the populated and fire-prone areas, the observed levoglucosan concentrations decline sharply and are typically less than 10 ng m^{-3} over marine and polar areas.[86−88] The lowest levoglucosan concentration reported (0.04 ng m^{-3}) was at Fraglione Camp, Antarctica.

Figure 2a also shows the annual mean particulate levoglucosan concentrations simulated by GEOS-Chem when atmospheric degradation processes are included. Similar to the observations, the model shows a wide range in particulate levoglucosan concentrations and a sharp decline away from the sources. The highest simulated annual mean levoglucosan concentrations are over the Siberian forest (400−1500 ng m^{-3}). The simulated levoglucosan concentrations generally exceed 500 ng m^{-3} over East Asia, South and Southeast Asia, central Africa, Eastern Europe, and the Canadian forests, reflecting the emissions from open fires or biofuel use. Over the oceans and the polar regions, the simulated concentrations are typically below 1 ng m^{-3}, with the exception of two marine sites in the Indian Ocean and in the Northwestern Pacific, which respectively experience continental influences from South Asia and Eastern China.[86] Simulated gas-phase levoglucosan concentrations show spatial distributions similar to particulate levoglucosan but are 2 to 3 orders of magnitude lower (10 to 10^{-4} ng m^{-3}, SI Figure S1). The simulated gas/particle partitioning ratios of levoglucosan in the surface air are between near-zero to 7%, consistent with constraints from the limited observations in the literature.[22]

Figure 3a more clearly demonstrate the sharp decline in particulate levoglucosan concentrations from near-source to remote sites, both in the observations and in our simulation with atmospheric degradation. Here the model is sampled at the locations and the months of measurements. The observed particulate levoglucosan concentrations are between 100 and 9000 ng m^{-3} in urban, rural, and forested sites but decrease to 0.04−27 ng m^{-3} at marine and polar sites. The model with atmospheric degradation generally reproduces the observed particulate levoglucosan concentration but has a slight low bias at near-source sites. The most significant low biases are at two urban sites (Bakersfield in California, U.S.; Geeveston in Tasmania, Australia) and two rural sites (Grove in Tasmania, Australia; Manjimup, Australia). These biases may be due to missing accounts of residential wood fuel use or prescribed forest burnings near the urban boundary, especially in Australia.[89] Over marine and polar areas, the model reproduces the observed low levoglucosan concentrations, except that the simulated concentrations are too low at two Antarctic sites. The measurements taken at these two sites were affected by biomass burning emissions from South America.[87]

If atmospheric degradation were not included in the model, the model would fail to reproduce the observed sharp concentration decline from near-source to remote sites (Figures 2b, 3a, and S2). Without atmospheric degradation, the simulated concentrations are still similar to the observed values at urban, rural, and forested sites. However, at marine and polar sites, the simulated concentrations would increase by 1-2 orders of magnitude when atmospheric degradation is turned off and thus much higher than the observed concentrations. As previously mentioned, we tune the levoglucosan emission factors to optimize agreement with observations at near-source sites (Section 2.2). However, that tuning would not affect the simulated concentration gradient. Figure S3 shows the ratios of simulated particulate levoglucosan concentrations with and without atmospheric degradation ($[L]/[L_{NOCHEM}]$). Degradation begins to take place near the sources. By the time levoglucosan particles are transported to the marine atmosphere, more than 50% have been removed. The degradation of levoglucosan is faster in summer than in winter (Figure S3). We also conduct sensitivity simulations using high-end values for the rates of aqueous and heterogeneous removal of levoglucosan and find that faster removal rates would lead to overestimation of the levoglucosan concentration gradient between near-source and remote sites (Text S2).

We further examine the impacts of levoglucosan's degradation on the particulate levoglucosan to OC concentration ratio ($[L]/[OC]$, Figure 3b) and the particulate levoglucosan to K^+ concentration ratio ($[L]/[K^+]$, Figure 3c). Without atmospheric degradation of levoglucosan, the removal of levoglucosan, OC, and K^+ in $PM_{2.5}$ would be mostly by the same processes (dry and wet deposition) and would occur at nearly the same rates (exceptions involve hydrophobic OC and semivolatile OC). As such, without levoglucosan degradation, the simulated $[L]/[OC]$ and $[L]/[K^+]$ are both relatively stable from near-source to remote sites. However, observations clearly show decreases of both $[L]/[OC]$ and $[L]/[K^+]$ from near-source to remote sites, corroborating the significant chemical degradation of levoglucosan in our simulation. Marine emissions of OC (not included in model), secondary production of OC (included in model), and larger marine emission of K^+ could increase the relative abundance of OC and K^+ at marine and polar sites.[21] However, it is unlikely that these factors alone could lead to the observed orders-of-magnitude decrease of $[L]/[OC]$ and $[L]/[K^+]$ from near-source to remote sites.

3.3. Impacts on Atmospheric Degradation the Global Budget of Levoglucosan. We compare the simulated global budget of atmospheric levoglucosan, with and without levoglucosan's atmospheric degradation (Table 2). If there were no atmospheric degradation of levoglucosan, the global emission of levoglucosan (3.8 Tg yr^{-1}) would be balanced mainly by wet deposition (3.1 Tg yr^{-1}) and to a smaller extent by dry deposition (0.7 Tg yr^{-1}). This balance would have led to a global burden of levoglucosan of 76 Gg and a mean lifetime of 7.3 days. With atmospheric degradation, chemical loss (3.1 Tg yr^{-1}) becomes the dominant sink of levoglucosan, mainly via aqueous oxidation by OH (2.6 Tg yr^{-1}) and NO_3 (0.35 Tg yr^{-1}). Heterogeneous oxidation (0.16 Tg yr^{-1}), gas-phase oxidation by OH (1.4×10^{-4} Tg yr^{-1}), and wet (0.43 Tg yr^{-1}) and dry (0.27 Tg yr^{-1}) depositions are relatively minor

https://doi.org/10.1021/acs.est.0c07313
Environ. Sci. Technol. XXXX, XXX, XXX−XXX

Table 2. Global Sources, Sinks, Burden, and Lifetime of Levoglucosan

	with atmospheric degradation	without atmospheric degradation
burden [Gg]	19	76
lifetime [day]	1.8	7.3
emission [Tg yr $^{-1}$]	3.8	3.8
open fire burning of vegetative matter [Tg yr $^{-1}$]	1.7	1.7
biofuel use [Tg yr $^{-1}$]	2.1	2.1
sink: aqueous-phase oxidation [Tg yr^{-1}]	2.9	
OH	2.6	
NO_3	0.35	
sink: heterogeneous oxidation [Tg yr^{-1}]	0.16	
O_3	0.15	
OH	0.012	
NO_3	4.5×10^{-4}	
N_2O_5	6.2×10^{-5}	
sink: gas-phase oxidation by OH [Tg yr^{-1}]	1.4×10^{-4}	
sink: dry deposition [Tg yr $^{-1}$]	0.27	0.74
sink: wet deposition [Tg yr $^{-1}$]	0.43	3.1

sinks. The global burden of atmospheric levoglucosan is 19 Gg. The atmospheric lifetime of levoglucosan (burden divided by total removal rate) is 1.8 days.

4. USE OF LEVOGLUCOSAN TO QUANTIFY BIOMASS BURNING CONTRIBUTION TO OC

4.1. Correction for Atmospheric Degradation of Particulate Levoglucosan. As discussed above, previous application of eq 1 did not account for levoglucosan's degradation and likely underestimated biomass burning's contribution to ambient OC. To correct such underestimation, we define a correction factor, x, representing the freshness of particulate levoglucosan at a receptor site:

$$x = [L]/[L_{NOCHEM}] \quad (10)$$

where [L] is the particulate levoglucosan concentration at the receptor site. $[L_{NOCHEM}]$ is the particulate levoglucosan concentration that would be at the receptor site, if there were no degradation. Eq 1 can thus be modified to account for the degradation of measured levoglucosan:

$$\text{contribution of biomass burning to OC}(\%) = \frac{\frac{1}{x}\left(\frac{[L]}{[OC]}\right)_{ambient}}{ER_{levoglucosan,OC}} \times 100\% \quad (11)$$

The value of x, which vary from 1 for air masses with fresh biomass burning emissions to 0 for extremely aged air masses, can be parametrized using our model results. Aqueous oxidation is the dominant sink for levoglucosan (Section 3.3). Thus, a logical choice would be to parametrize x as a function of the simulated molar ratio between SO_2 and the sum of SO_2 and sulfate in the sampled air mass, $[SO_2]/([SO_2] + [SO_4^{2-}])$, because sulfate is largely produced by the aqueous oxidation of SO_2. However, because SO_2 (mostly emitted from coal-burning) is not coemitted with levoglucosan, x is not highly correlated with $[SO_2]/([SO_2]+[SO_4^{2-}])$ on a global scale (SI Figure S4a).

We next parametrize x as a function of the simulated molar ratio of NO_x (≡NO + NO_2) to NO_y (≡NO_x + HNO_2 + HNO_3 + HNO_4 + peroxyacetyl nitrate + peroxymethacroyl nitrate), which is a widely used indicator for atmospheric aging.[90] We find a relatively good linear fit (R = 0.78, SI Figure S5a):

$$x = 0.94 \cdot \frac{[NO_x]}{[NO_y]} - 0.09 \quad (12)$$

However, atmospheric NO_x has many sources; only 20% of NO_x is emitted from biomass burning on a global scale.[91] In the remote marine atmosphere, NO_x is more likely from lightning.[92] As such, over the oceans, the $([NO_x]/[NO_y])$ ratio does not reflect the aging of an air mass during its transport from a biomass burning or continental source.

Finally, we parametrize x using another biomass burning tracer, K^+. Here we also find some interference with the use of total K^+, because dust and sea salt are also important regional sources of K^+ (SI Figure S4b). However, if we use only the concentrations of K^+ emitted from biomass burning ($[K^+_{BB}]$), x can be well-fitted as a function of the ratio of [L]/ $[K^+_{BB}]$ (R = 0.84, SI Figure S5b). This relationship reflect the aging of an air mass during its transport from a biomass burning source:

$$x = 0.18 \cdot \frac{[L]}{[K^+_{BB}]} + 0.08 \quad (13)$$

4.2. Application to Particulate Levoglucosan Measurements at Lin'an, China and Chichijima, Japan. We apply our parametrizations to the particulate levoglucosan measurements in Lin'an, China (a rural site in central eastern China)[80] and Chichijima, Japan (an island site in the North Pacific),[93−95] to demonstrate the improved use of levoglucosan measurements for aerosol source apportionment. Intensive wheat straw burning is known to be a major source of aerosols over central eastern China in June,[96] yet Liang et al.[80] found that levoglucosan concentrations were not elevated at Lin'an in June 2015. They inferred that the site was not significantly affected by biomass burning in June 2015. We contend here that the levogluocsan in their sampled air may have significantly degraded. We raise these clues: (1) the levoglucosan measured at this site was significantly correlated with OC (R^2 between 0.52 and 0.71) and nonsea-salt K^+ (R^2 between 0.49 and 0.66) and not correlated with elemental carbon in all seasons, indicating significant contributions of biomass burning to the local OC and nonsea-salt K^+ year-round. (2) The measured levoglucosan to OC concentration ratios ([L]/[OC]) in summer was 0.0028, 1−2 orders of magnitude smaller than the emission ratios ($ER_{levoglucosan,OC}$ between 0.05 and 0.12) for Asian crop residue reported from burning chambers.[97] (3) The measured levoglucosan to OC concentration ratio was lowest in summer and highest in winter, potentially reflecting more efficient aqueous oxidation of levoglucosan in summer. Using eq 1 and ignoring levoglucosan's degradation, one would estimate a 2.3−5.6% contribution of biomass burning to local OC. However, by applying eqs 11 and 13 to correct for levoglucosan's degradation, we estimate a 14−33% contribution of biomass burning to the local OC, more consistent with the observed high correlation between levoglucosan and OC.

At Chichijima, Japan, Mochida et al.[21] proposed that the observed low particulate levoglucosan concentrations in aged Asian outflows in summer were due to the levoglucosan's degradation during transport. Our sensitivity simulations

https://doi.org/10.1021/acs.est.0c07313
Environ. Sci. Technol. XXXX, XXX, XXX−XXX

support their point of view. Our model reproduces the observed particulate levoglucosan concentrations (0.03−1.43 ng m^{-3}), as well as the observed [L]/[OC] (0.05−0.6) and [L]/[nonsea-salt K^+] (0.01−0.09) ratios at Chichijima in summer 2008[93] when levoglucosan's degradation is considered. The model would overestimate these values by 2−3 orders of magnitude, if levoglucosan's degradation were not included. Using eq 1 and ignoring atmospheric degradation, one would infer that biomass burning only contributes 0.3−0.8% of the summertime ambient OC at Chichijima. However, using eqs 11−13 to correct for levoglucosan's degradation, we estimate that biomass burning contributed 3.4−8.3% of the summertime ambient OC at Chichijima.

5. DISCUSSION

Our comparison of observed and simulated levoglucosan concentrations at global sites corroborate the significant atmospheric degradation of levoglucosan. Such significant degradation should be considered when using levoglucosan to quantify the contribution of biomass burning to ambient aerosols. We achieve this by empirically representing the freshness of the levoglucosan at a receptor site using either the observed $[NO_x]/[NO_y]$ ratio (eq 12) or the observed $[L]/[K^+_{BB}]$ ratio (eq 13). At sites where K^+ was dominated by biomass burning, eq 13 would be a better choice. For general quantification of atmospheric aging, eq 12 can be used. Further studies are needed to better constrain the degradation rates of levoglucosan in the atmosphere to improve the use of levoglucosan as a quantitative pyrogenic tracer for studies of air quality and climate.

■ ASSOCIATED CONTENT

Supporting Information

The Supporting Information is available free of charge at https://pubs.acs.org/doi/10.1021/acs.est.0c07313.

Text, Tables and Figures as noted in the text (PDF)

■ AUTHOR INFORMATION

Corresponding Authors

Tzung-May Fu − *School of Environmental Sciences and Engineering and Shenzhen Institute of Sustainable Development, Southern University of Science and Technology, Shenzhen, Guangdong Province 518055, China;* orcid.org/0000-0002-8556-7326; Email: fuzm@sustech.edu.cn

Jian Zhen Yu − *Division of Environment and Sustainability and Department of Chemistry, Hong Kong University of Science and Technology, Hong Kong 999077, China;* orcid.org/0000-0002-6165-6500; Email: chjianyu@ust.hk

Authors

Yumin Li − *School of Environmental Sciences and Engineering, Southern University of Science and Technology, Shenzhen, Guangdong Province 518055, China; Division of Environment and Sustainability, Hong Kong University of Science and Technology, Hong Kong 999077, China;* orcid.org/0000-0002-5686-3249

Xu Feng − *School of Environmental Sciences and Engineering, Southern University of Science and Technology, Shenzhen, Guangdong Province 518055, China; Department of Atmospheric and Oceanic Sciences, School of Physics, Peking University, Beijing 100871, China*

Lijuan Zhang − *School of Environmental Sciences and Engineering, Southern University of Science and Technology, Shenzhen, Guangdong Province 518055, China; Department of Atmospheric and Oceanic Sciences, School of Physics, Peking University, Beijing 100871, China*

Jing Chen − *Institute of Low Temperature Science, Hokkaido University, Sapporo 060-0819, Japan; School of Environmental Science and Engineering, Tianjin University, Tianjin 300072, China*

Suresh Kumar Reddy Boreddy − *Space Physics Laboratory, Vikram Sarabhai Space Centre, Indian Space Research Organization, Thiruvananthapuram 695022, India; Institute of Low Temperature Science, Hokkaido University, Sapporo 060-0819, Japan;* orcid.org/0000-0002-0619-2942

Kimitaka Kawamura − *Institute of Low Temperature Science, Hokkaido University, Sapporo 060-0819, Japan; Chubu Institute for Advanced Studies, Chubu University, Kasugai 487-8501, Japan;* orcid.org/0000-0003-1190-3726

Pingqing Fu − *School of Earth System Science, Tianjin University, Tianjin 300072, China;* orcid.org/0000-0001-6249-2280

Xin Yang − *School of Environmental Sciences and Engineering and Shenzhen Institute of Sustainable Development, Southern University of Science and Technology, Shenzhen, Guangdong Province 518055, China;* orcid.org/0000-0002-9173-1188

Lei Zhu − *School of Environmental Sciences and Engineering and Shenzhen Institute of Sustainable Development, Southern University of Science and Technology, Shenzhen, Guangdong Province 518055, China*

Zhenzhong Zeng − *School of Environmental Sciences and Engineering and Shenzhen Institute of Sustainable Development, Southern University of Science and Technology, Shenzhen, Guangdong Province 518055, China*

Complete contact information is available at: https://pubs.acs.org/10.1021/acs.est.0c07313

Notes

The authors declare no competing financial interest.

■ ACKNOWLEDGMENTS

This work was supported by the National Natural Science Foundation of China (41975158) and the Shenzhen Science and Technology Innovation Committee (KCXFZ202002011008038). Computational resources were provided by the Center for Computational Science and Engineering at the Southern University of Science and Technology. We acknowledge the measurement compilation of Bhattarai et al. (2019), on which SI Table S1 is largely based.

■ REFERENCES

(1) Suciu, L. G.; Masiello, C. A.; Griffin, R. J. Anhydrosugars as tracers in the Earth system. *Biogeochemistry* **2019**, *146* (3), 209−256.

(2) Simoneit, B. R. T.; Schauer, J. J.; Nolte, C. G.; Oros, D. R.; Elias, V. O.; Fraser, M. P.; Rogge, W. F.; Cass, G. R. Levoglucosan, a tracer for cellulose in biomass burning and atmospheric particles. *Atmos. Environ.* **1999**, *33* (2), 173−182.

(3) Bond, T. C.; Streets, D. G.; Yarber, K. F.; Nelson, S. M.; Woo, J. H.; Klimont, Z. A technology-based global inventory of black and

organic carbon emissions from combustion. *J. Geophys. Res.* **2004**, *109* (D14), D14203.
(4) van der Werf, G. R.; Randerson, J. T.; Giglio, L.; van Leeuwen, T. T.; Chen, Y.; Rogers, B. M.; Mu, M. Q.; van Marle, M. J. E.; Morton, D. C.; Collatz, G. J.; Yokelson, R. J.; Kasibhatla, P. S. Global fire emissions estimates during 1997−2016. *Earth System Science Data* **2017**, *9* (2), 697−720.
(5) Andreae, M. O. Emission of trace gases and aerosols from biomass burning - an updated assessment. *Atmos. Chem. Phys.* **2019**, *19* (13), 8523−8546.
(6) Fu, P. Q.; Kawamura, K.; Chen, J.; Miyazaki, Y. Secondary production of organic aerosols from biogenic VOCs over Mt. Fuji, Japan. *Environ. Sci. Technol.* **2014**, *48* (15), 8491−8497.
(7) Ho, K. F.; Engling, G.; Ho, S. S. H.; Huang, R. J.; Lai, S. C.; Cao, J. J.; Lee, S. C. Seasonal variations of anhydrosugars in PM2.5 in the Pearl River Delta Region, China. *Tellus, Ser. B* **2014**, *66*, 22577.
(8) Zheng, L. S.; Yang, X. Y.; Lai, S. C.; Ren, H.; Yue, S. Y.; Zhang, Y. Y.; Huang, X.; Gao, Y. G.; Sun, Y. L.; Wang, Z. F.; Fu, P. Q. Impacts of springtime biomass burning in the northern Southeast Asia on marine organic aerosols over the Gulf of Tonkin, China. *Environ. Pollut.* **2018**, *237*, 285−297.
(9) Li, X. R.; Wen, T. X.; Xin, J. Y.; Liu, Z. R.; Liu, S. Q.; Li, D.; Zhang, R. Y.; Wang, Y. F.; Wang, Y. S. Spatial and seasonal variations of sugars (alcohol) in China: Emerging results from the CARE-China network. *Atmos. Environ.* **2019**, *209*, 136−143.
(10) Zhang, Q.; Jimenez, J. L.; Canagaratna, M. R.; Allan, J. D.; Coe, H.; Ulbrich, I.; Alfarra, M. R.; Takami, A.; Middlebrook, A. M.; Sun, Y. L.; Dzepina, K.; Dunlea, E.; Docherty, K.; DeCarlo, P. F.; Salcedo, D.; Onasch, T.; Jayne, J. T.; Miyoshi, T.; Shimono, A.; Hatakeyama, S.; Takegawa, N.; Kondo, Y.; Schneider, J.; Drewnick, F.; Borrmann, S.; Weimer, S.; Demerjian, K.; Williams, P.; Bower, K.; Bahreini, R.; Cottrell, L.; Griffin, R. J.; Rautiainen, J.; Sun, J. Y.; Zhang, Y. M.; Worsnop, D. R. Ubiquity and dominance of oxygenated species in organic aerosols in anthropogenically-influenced Northern Hemisphere midlatitudes. *Geophys. Res. Lett.* **2007**, *34* (13), 6. L13801
(11) Hoffmann, D.; Tilgner, A.; Iinuma, Y.; Herrmann, H. Atmospheric stability of levoglucosan: a detailed laboratory and modeling study. *Environ. Sci. Technol.* **2010**, *44* (2), 694−699.
(12) Kessler, S. H.; Smith, J. D.; Che, D. L.; Worsnop, D. R.; Wilson, K. R.; Kroll, J. H. Chemical sinks of organic aerosol: kinetics and products of the heterogeneous oxidation of erythritol and levoglucosan. *Environ. Sci. Technol.* **2010**, *44* (18), 7005−7010.
(13) Knopf, D. A.; Forrester, S. M.; Slade, J. H. Heterogeneous oxidation kinetics of organic biomass burning aerosol surrogates by O-3, NO2, N2O5, and NO3. *Phys. Chem. Chem. Phys.* **2011**, *13* (47), 21050−21062.
(14) Slade, J. H.; Knopf, D. A. Multiphase OH oxidation kinetics of organic aerosol: The role of particle phase state and relative humidity. *Geophys. Res. Lett.* **2014**, *41* (14), 5297−5306.
(15) Gensch, I.; Sang-Arlt, X. F.; Laumer, W.; Chan, C. Y.; Engling, G.; Rudolph, J.; Kiendler-Scharr, A. Using delta C-13 of levoglucosan as a chemical clock. *Environ. Sci. Technol.* **2018**, *52* (19), 11094−11101.
(16) Bai, J.; Sun, X. M.; Zhang, C. X.; Xu, Y. S.; Qi, C. S. The OH-initiated atmospheric reaction mechanism and kinetics for levoglucosan emitted in biomass burning. *Chemosphere* **2013**, *93* (9), 2004−2010.
(17) Yang, C.; Zhang, C. Y.; Luo, X. S.; Liu, X. Y.; Cao, F.; Zhang, Y. L. Isomerization and degradation of levoglucosan via the Photo-Fenton Process: insights from aqueous-phase experiments and atmospheric particulate matter. *Environ. Sci. Technol.* **2020**, *54* (19), 11789−11797.
(18) Sang, X. F.; Gensch, I.; Laumer, W.; Kammer, B.; Chan, C. Y.; Engling, G.; Wahner, A.; Wissel, H.; Kiendler-Scharr, A. Stable carbon isotope ratio analysis of anhydrosugars in biomass burning aerosol particles from source samples. *Environ. Sci. Technol.* **2012**, *46* (6), 3312−3318.
(19) Lai, C. Y.; Liu, Y. C.; Ma, J. Z.; Ma, Q. X.; He, H. Degradation kinetics of levoglucosan initiated by hydroxyl radical under different environmental conditions. *Atmos. Environ.* **2014**, *91*, 32−39.
(20) Arangio, A. M.; Slade, J. H.; Berkemeier, T.; Poschl, U.; Knopf, D. A.; Shiraiwa, M. Multiphase chemical kinetics of OH radical uptake by molecular organic markers of biomass burning aerosols: humidity and temperature dependence, surface reaction, and bulk diffusion. *J. Phys. Chem. A* **2015**, *119* (19), 4533−4544.
(21) Mochida, M.; Kawamura, K.; Fu, P. Q.; Takemura, T. Seasonal variation of levoglucosan in aerosols over the western North Pacific and its assessment as a biomass-burning tracer. *Atmos. Environ.* **2010**, *44* (29), 3511−3518.
(22) Xie, M. J.; Hannigan, M. P.; Barsanti, K. C. Gas/particle partitioning of 2-methyltetrols and levoglucosan at an urban site in Denver. *Environ. Sci. Technol.* **2014**, *48* (5), 2835−2842.
(23) Arakaki, T.; Anastasio, C.; Kuroki, Y.; Nakajima, H.; Okada, K.; Kotani, Y.; Handa, D.; Azechi, S.; Kimura, T.; Tsuhako, A.; Miyagi, Y. A General scavenging rate constant for reaction of hydroxyl radical with organic carbon in atmospheric waters. *Environ. Sci. Technol.* **2013**, *47* (15), 8196−8203.
(24) Bianco, A.; Passananti, M.; Brigante, M.; Mailhot, G. Photochemistry of the cloud aqueous phase: a review. *Molecules* **2020**, *25* (2), 423.
(25) Hennigan, C. J.; Sullivan, A. P.; Collett, J. L.; Robinson, A. L. Levoglucosan stability in biomass burning particles exposed to hydroxyl radicals. *Geophys. Res. Lett.* **2010**, *37*, L09806.
(26) Slade, J. H.; Knopf, D. A. Heterogeneous OH oxidation of biomass burning organic aerosol surrogate compounds: assessment of volatilisation products and the role of OH concentration on the reactive uptake kinetics. *Phys. Chem. Chem. Phys.* **2013**, *15* (16), 5898−5915.
(27) Suciu, L. G.; Griffin, R. J.; Masiello, C. A. A zero-dimensional view of atmospheric degradation of levoglucosan (LEVCHEM_v1) using numerical chamber simulations. *Geosci. Model Dev. Discuss.* **2020**, *2020*, 1−23.
(28) Bey, I.; Jacob, D. J.; Yantosca, R. M.; Logan, J. A.; Field, B. D.; Fiore, A. M.; Li, Q. B.; Liu, H. G. Y.; Mickley, L. J.; Schultz, M. G. Global modeling of tropospheric chemistry with assimilated meteorology: Model description and evaluation. *Journal of Geophysical Research-Atmospheres* **2001**, *106* (D19), 23073−23095.
(29) Park, R. J.; Jacob, D. J.; Field, B. D.; Yantosca, R. M.; Chin, M. Natural and transboundary pollution influences on sulfate-nitrate-ammonium aerosols in the United States: Implications for policy. *J. Geophys. Res.* **2004**, *109* (D15), D15204.
(30) Parrella, J. P.; Jacob, D. J.; Liang, Q.; Zhang, Y.; Mickley, L. J.; Miller, B.; Evans, M. J.; Yang, X.; Pyle, J. A.; Theys, N.; Van Roozendael, M. Tropospheric bromine chemistry: implications for present and pre-industrial ozone and mercury. *Atmos. Chem. Phys.* **2012**, *12* (15), 6723−6740.
(31) Mao, J. Q.; Paulot, F.; Jacob, D. J.; Cohen, R. C.; Crounse, J. D.; Wennberg, P. O.; Keller, C. A.; Hudman, R. C.; Barkley, M. P.; Horowitz, L. W. Ozone and organic nitrates over the eastern United States: Sensitivity to isoprene chemistry. *Journal of Geophysical Research-Atmospheres* **2013**, *118* (19), 11256−11268.
(32) Park, R. J.; Jacob, D. J.; Chin, M.; Martin, R. V. Sources of carbonaceous aerosols over the United States and implications for natural visibility. *J. Geophys. Res.* **2003**, *108* (D12), 4355.
(33) Fairlie, T. D.; Jacob, D. J.; Park, R. J. The impact of transpacific transport of mineral dust in the United States. *Atmos. Environ.* **2007**, *41* (6), 1251−1266.
(34) Jaeglé, L.; Quinn, P. K.; Bates, T. S.; Alexander, B.; Lin, J. T. Global distribution of sea salt aerosols: new constraints from in situ and remote sensing observations. *Atmos. Chem. Phys.* **2011**, *11* (7), 3137−3157.
(35) Pai, S. J.; Heald, C. L.; Pierce, J. R.; Farina, S. C.; Marais, E. A.; Jimenez, J. L.; Campuzano-Jost, P.; Nault, B. A.; Middlebrook, A. M.; Coe, H.; Shilling, J. E.; Bahreini, R.; Dingle, J. H.; Vu, K. An evaluation of global organic aerosol schemes using airborne observations. *Atmos. Chem. Phys.* **2020**, *20* (5), 2637−2665.

https://doi.org/10.1021/acs.est.0c07313
Environ. Sci. Technol. XXXX, XXX, XXX−XXX

(36) Wesely, M. L. Parameterization of surface resistances to gaseous dry deposition in regional-scale numerical models. *Atmos. Environ.* **1989**, *23* (6), 1293−1304.
(37) Zhang, L. M.; Gong, S. L.; Padro, J.; Barrie, L. A size-segregated particle dry deposition scheme for an atmospheric aerosol module. *Atmos. Environ.* **2001**, *35* (3), 549−560.
(38) Liu, H. Y.; Jacob, D. J.; Bey, I.; Yantosca, R. M. Constraints from Pb-210 and Be-7 on wet deposition and transport in a global three-dimensional chemical tracer model driven by assimilated meteorological fields. *Journal of Geophysical Research-Atmospheres* **2001**, *106* (D11), 12109−12128.
(39) Amos, H. M.; Jacob, D. J.; Holmes, C. D.; Fisher, J. A.; Wang, Q.; Yantosca, R. M.; Corbitt, E. S.; Galarneau, E.; Rutter, A. P.; Gustin, M. S.; Steffen, A.; Schauer, J. J.; Graydon, J. A.; St Louis, V. L.; Talbot, R. W.; Edgerton, E. S.; Zhang, Y.; Sunderland, E. M. Gas-particle partitioning of atmospheric Hg(II) and its effect on global mercury deposition. *Atmos. Chem. Phys.* **2012**, *12* (1), 591−603.
(40) Hoesly, R. M.; Smith, S. J.; Feng, L. Y.; Klimont, Z.; Janssens-Maenhout, G.; Pitkanen, T.; Seibert, J. J.; Vu, L.; Andres, R. J.; Bolt, R. M.; Bond, T. C.; Dawidowski, L.; Kholod, N.; Kurokawa, J.; Li, M.; Liu, L.; Lu, Z. F.; Moura, M. C. P.; O'Rourke, P. R.; Zhang, Q. Historical (1750−2014) anthropogenic emissions of reactive gases and aerosols from the Community Emissions Data System (CEDS). *Geosci. Model Dev.* **2018**, *11* (1), 369−408.
(41) Bhattarai, H.; Saikawa, E.; Wan, X.; Zhu, H. X.; Ram, K.; Gao, S. P.; Kang, S. C.; Zhang, Q. G.; Zhang, Y. L.; Wu, G. M.; Wang, X. P.; Kawamura, K.; Fu, P. Q.; Cong, Z. Y. Levoglucosan as a tracer of biomass burning: Recent progress and perspectives. *Atmos. Res.* **2019**, *220*, 20−33.
(42) Wu, J.; Kong, S.; Zeng, X.; Cheng, Y.; Yan, Q.; Zheng, H.; Yan, Y.; Zheng, S.; Liu, D.; Zhang, X.; Fu, P.; Wang, S.; Qi, S., First high-resolution emission inventory of levoglucosan for biomass burning and non-biomass burning sources in China. *Environ. Sci. Technol.* **2021**.551497
(43) Yan, C. Q.; Zheng, M.; Sullivan, A. P.; Shen, G. F.; Chen, Y. J.; Wang, S. X.; Zhao, B.; Cai, S. Y.; Desyaterik, Y.; Li, X. Y.; Zhou, T.; Gustafsson, O.; Collett, J. L. Residential coal combustion as a cource of levoglucosan in China. *Environ. Sci. Technol.* **2018**, *52* (3), 1665−1674.
(44) Randerson, J. T.; Thompson, M. V.; Malmstrom, C. M.; Field, C. B.; Fung, I. Y. Substrate limitations for heterotrophs: Implications for models that estimate the seasonal cycle of atmospheric CO2. *Global Biogeochemical Cycles* **1996**, *10* (4), 585−602.
(45) Randerson, J. T.; Chen, Y.; van der Werf, G. R.; Rogers, B. M.; Morton, D. C. Global burned area and biomass burning emissions from small fires. *Journal of Geophysical Research-Biogeosciences* **2012**, *117*, G04012.
(46) Marais, E. A.; Wiedinmyer, C. Air quality impact of diffuse and inefficient combustion emissions in Africa (DICE-Africa). *Environ. Sci. Technol.* **2016**, *50* (19), 10739−10745.
(47) Bond, T. C.; Bhardwaj, E.; Dong, R.; Jogani, R.; Jung, S. K.; Roden, C.; Streets, D. G.; Trautmann, N. M. Historical emissions of black and organic carbon aerosol from energy-related combustion, 1850−2000. *Global Biogeochemical Cycles* **2007**, *21* (2), Gb2018.
(48) United Nations (UN) Data Portal, EnergyStatistics Database. United Nations Statistics Division (UNSD): 2015. http://data.un.org/Explorer.aspx?d=EDATA.
(49) Wang, X. Y.; Meyer, C. P.; Reisen, F.; Keywood, M.; Thai, P. K.; Hawker, D. W.; Powell, J.; Mueller, J. F. Emission factors for selected semivolatile organic chemicals from burning of tropical biomass fuels and estimation of annual Australian emissions. *Environ. Sci. Technol.* **2017**, *51* (17), 9644−9652.
(50) Graham, B.; Mayol-Bracero, O. L.; Guyon, P.; Roberts, G. C.; Decesari, S.; Facchini, M. C.; Artaxo, P.; Maenhaut, W.; Koll, P.; Andreae, M. O. Water-soluble organic compounds in biomass burning aerosols over Amazonia - 1. Characterization by NMR and GC-MS. *J. Geophys. Res.* **2002**, *107* (D20), 8047.
(51) Landis, M. S.; Edgerton, E. S.; White, E. M.; Wentworth, G. R.; Sullivan, A. P.; Dillner, A. M. The impact of the 2016 Fort McMurray Horse River Wildfire on ambient air pollution levels in the Athabasca Oil Sands Region, Alberta, Canada. *Sci. Total Environ.* **2018**, *618*, 1665−1676.
(52) Jayarathne, T.; Stockwell, C. E.; Bhave, P. V.; Praveen, P. S.; Rathnayake, C. M.; Islam, M. R.; Panday, A. K.; Adhikari, S.; Maharjan, R.; Goetz, J. D.; DeCarlo, P. F.; Saikawa, E.; Yokelson, R. J.; Stone, E. A. Nepal ambient monitoring and source testing experiment (NAMaSTE): emissions of particulate matter from wood- and dung-fueled cooking fires, garbage and crop residue burning, brick kilns, and other sources. *Atmos. Chem. Phys.* **2018**, *18* (3), 2259−2286.
(53) Oros, D. R.; Simoneit, B. R. T. Identification and emission factors of molecular tracers in organic aerosols from biomass burning Part 2. Deciduous trees. *Appl. Geochem.* **2001**, *16* (13), 1545−1565.
(54) Oros, D. R.; bin Abas, M. R.; Omar, N.; Rahman, N. A.; Simoneit, B. R. T. Identification and emission factors of molecular tracers in organic aerosols from biomass burning: Part 3. Grasses. *Appl. Geochem.* **2006**, *21* (6), 919−940.
(55) Iinuma, Y.; Bruggemann, E.; Gnauk, T.; Muller, K.; Andreae, M. O.; Helas, G.; Parmar, R.; Herrmann, H. Source characterization of biomass burning particles: The combustion of selected European conifers, African hardwood, savanna grass, and German and Indonesian peat. *Journal of Geophysical Research-Atmospheres* **2007**, *112* (D8), D08209.
(56) Munchak, L. A.; Schichtel, B. A.; Sullivan, A. P.; Holden, A. S.; Kreidenweis, S. M.; Malm, W. C.; Collett, J. L. Development of wildland fire particulate smoke marker to organic carbon emission ratios for the conterminous United States. *Atmos. Environ.* **2011**, *45* (2), 395−403.
(57) Chantara, S.; Thepnuan, D.; Wiriya, W.; Prawan, S.; Tsai, Y. I. Emissions of pollutant gases, fine particulate matters and their significant tracers from biomass burning in an open-system combustion chamber. *Chemosphere* **2019**, *224*, 407−416.
(58) Hall, D.; Wu, C. Y.; Hsu, Y. M.; Stormer, J.; Engling, G.; Capeto, K.; Wang, J.; Brown, S.; Li, H. W.; Yu, K. M. PAHs, carbonyls, VOCs and PM2.5 emission factors for pre-harvest burning of Florida sugarcane. *Atmos. Environ.* **2012**, *55*, 164−172.
(59) Otto, A.; Gondokusumo, R.; Simpson, M. J. Characterization and quantification of biomarkers from biomass burning at a recent wildfire site in Northern Alberta, Canada. *Appl. Geochem.* **2006**, *21* (1), 166−183.
(60) Ridley, D. A.; Heald, C. L.; Pierce, J. R.; Evans, M. J. Toward resolution-independent dust emissions in global models: Impacts on the seasonal and spatial distribution of dust. *Geophys. Res. Lett.* **2013**, *40* (11), 2873−2877.
(61) Fairlie, T. D.; Jacob, D. J.; Dibb, J. E.; Alexander, B.; Avery, M. A.; van Donkelaar, A.; Zhang, L. Impact of mineral dust on nitrate, sulfate, and ozone in transpacific Asian pollution plumes. *Atmos. Chem. Phys.* **2010**, *10* (8), 3999−4012.
(62) Philip, S.; Martin, R. V.; Snider, G.; Weagle, C. L.; van Donkelaar, A.; Brauer, M.; Henze, D. K.; Klimont, Z.; Venkataraman, C.; Guttikunda, S. K.; Zhang, Q. Anthropogenic fugitive, combustion and industrial dust is a significant, underrepresented fine particulate matter source in global atmospheric models. *Environ. Res. Lett.* **2017**, *12* (4), No. 044018.
(63) Skorbiłowicz, M.; Skorbiłowicz, E. Content of calcium, magnesium, sodium and potassium in the street dust from the area of Białystok (Poland). *Journal of Ecological Engineering* **2019**, *20* (10), 125−131.
(64) Karavoltsos, S.; Sakellari, A.; Bakeas, E.; Bekiaris, G.; Plavsic, M.; Proestos, C.; Zinelis, S.; Koukoulakis, K.; Diakos, I.; Dassenakis, M.; Kalogeropoulos, N. Trace elements, polycyclic aromatic hydrocarbons, mineral composition, and FT-IR characterization of unrefined sea and rock salts: environmental interactions. *Environ. Sci. Pollut. Res.* **2020**, *27* (10), 10857−10868.
(65) White, W. H. Chemical markers for sea salt in IMPROVE aerosol data. *Atmos. Environ.* **2008**, *42* (2), 261−274.

https://doi.org/10.1021/acs.est.0c07313
Environ. Sci. Technol. XXXX, XXX, XXX−XXX

(66) Pye, H. O. T.; Seinfeld, J. H. A global perspective on aerosol from low-volatility organic compounds. *Atmos. Chem. Phys.* **2010**, *10* (9), 4377−4401.
(67) Zhao, Y. L.; Kreisberg, N. M.; Worton, D. R.; Isaacman, G.; Weber, R. J.; Liu, S.; Day, D. A.; Russell, L. M.; Markovic, M. Z.; VandenBoer, T. C.; Murphy, J. G.; Hering, S. V.; Goldstein, A. H. Insights into Secondary Organic Aerosol Formation Mechanisms from Measured Gas/Particle Partitioning of Specific Organic Tracer Compounds. *Environ. Sci. Technol.* **2013**, *47* (8), 3781−3787.
(68) Booth, A. M.; Montague, W. J.; Barley, M. H.; Topping, D. O.; McFiggans, G.; Garforth, A.; Percival, C. J. Solid state and sub-cooled liquid vapour pressures of cyclic aliphatic dicarboxylic acids. *Atmos. Chem. Phys.* **2011**, *11* (2), 655−665.
(69) Parshintsev, J.; Ruiz-Jimenez, J.; Petaja, T.; Hartonen, K.; Kulmala, M.; Riekkola, M. L. Comparison of quartz and Teflon filters for simultaneous collection of size-separated ultrafine aerosol particles and gas-phase zero samples. *Anal. Bioanal. Chem.* **2011**, *400* (10), 3527−3535.
(70) Levin, Z.; Teller, A.; Ganor, E.; Graham, B.; Andreae, M. O.; Maenhaut, W.; Falkovich, A. H.; Rudich, Y. Role of aerosol size and composition in nucleation scavenging within clouds in a shallow cold front. *Journal of Geophysical Research-Atmospheres* **2003**, *108* (D22), 4700.
(71) Li, X.; Jiang, L.; Hoa, L. P.; Lyu, Y.; Xu, T. T.; Yang, X.; Iinuma, Y.; Chen, J. M.; Herrmann, H. Size distribution of particle-phase sugar and nitrophenol tracers during severe urban haze episodes in Shanghai. *Atmos. Environ.* **2016**, *145*, 115−127.
(72) Xu, S. F.; Ren, L. J.; Lang, Y. C.; Hou, S. J.; Ren, H.; Wei, L. F.; Wu, L. B.; Deng, J. J.; Hu, W.; Pan, X. L.; Sun, Y. L.; Wang, Z. F.; Su, H.; Cheng, Y. F.; Fu, P. Q. Molecular markers of biomass burning and primary biological aerosols in urban Beijing: size distribution and seasonal variation. *Atmos. Chem. Phys.* **2020**, *20* (6), 3623−3644.
(73) Zamora, I. R.; Tabazadeh, A.; Golden, D. M.; Jacobson, M. Z. Hygroscopic growth of common organic aerosol solutes, including humic substances, as derived from water activity measurements. *Journal of Geophysical Research-Atmospheres* **2011**, *116*, D23207.
(74) Thomas, K.; Volz-Thomas, A.; Mihelcic, D.; Smit, H. G. J.; Kley, D. On the exchange of NO3 radicals with aqueous solutions: Solubility and sticking coefficient. *J. Atmos. Chem.* **1998**, *29* (1), 17−43.
(75) Jacob, D. J.; Field, B. D.; Li, Q. B.; Blake, D. R.; de Gouw, J.; Warneke, C.; Hansel, A.; Wisthaler, A.; Singh, H. B.; Guenther, A. Global budget of methanol: Constraints from atmospheric observations. *Journal of Geophysical Research-Atmospheres* **2005**, *110* (D8), D08303.
(76) Tilgner, A.; Brauer, P.; Wolke, R.; Herrmann, H. Modelling multiphase chemistry in deliquescent aerosols and clouds using CAPRAM3.0i. *J. Atmos. Chem.* **2013**, *70* (3), 221−256.
(77) Fuchs, N. A.; Sutugin, A. G. High-Dispersed Aerosols. In *Topics in Current Aerosol Research*; International Reviews in Aerosol Physics and Chemistry, Elsevier, 1971; p 1.
(78) Shen, Z. X.; Zhang, Q.; Cao, J. J.; Zhang, L. M.; Lei, Y. L.; Huang, Y.; Huang, R. J.; Gao, J. J.; Zhao, Z. Z.; Zhu, C. S.; Yin, X. L.; Zheng, C. L.; Xu, H. M.; Liu, S. X. Optical properties and possible sources of brown carbon in PM2.5 over Xi'an, China. *Atmos. Environ.* **2017**, *150*, 322−330.
(79) Liu, X. Y.; Zhang, Y. L.; Peng, Y. R.; Xu, L. L.; Zhu, C. M.; Cao, F.; Zhai, X. Y.; Haque, M. M.; Yang, C.; Chang, Y. H.; Huang, T.; Xu, Z. F.; Bao, M. Y.; Zhang, W. Q.; Fan, M. Y.; Lee, X. H. Chemical and optical properties of carbonaceous aerosols in Nanjing, eastern China: regionally transported biomass burning contribution. *Atmos. Chem. Phys.* **2019**, *19* (17), 11213−11233.
(80) Liang, L. L.; Engling, G.; Cheng, Y.; Liu, X. Y.; Du, Z. Y.; Ma, Q. L.; Zhang, X. Y.; Sun, J. Y.; Xu, W. Y.; Liu, C.; Zhang, G.; Xu, H., Biomass burning impacts on ambient aerosol at a background site in East China: Insights from a yearlong study. *Atmos. Res.* **2020**, *231*, UNSP 104660.104660
(81) Simpson, C. D.; Dills, R. L.; Katz, B. S.; Kalman, D. A. Determination of levoglucosan in atmospheric fine particulate matter. *J. Air Waste Manage. Assoc.* **2004**, *54* (6), 689−694.
(82) Larsen, R. K.; Schantz, M. M.; Wise, S. A. Determination of levoglucosan in particulate matter reference materials. *Aerosol Sci. Technol.* **2006**, *40* (10), 781−787.
(83) Giannoni, M.; Martellini, T.; Del Bubba, M.; Gambaro, A.; Zangrando, R.; Chiari, M.; Lepri, L.; Cincinelli, A. The use of levoglucosan for tracing biomass burning in PM2.5 samples in Tuscany (Italy). *Environ. Pollut.* **2012**, *167*, 7−15.
(84) Urban, R. C.; Lima-Souza, M.; Caetano-Silva, L.; Queiroz, M. E. C.; Nogueira, R. F. P.; Allen, A. G.; Cardoso, A. A.; Held, G.; Campos, M. Use of levoglucosan, potassium, and water-soluble organic carbon to characterize the origins of biomass-burning aerosols. *Atmos. Environ.* **2012**, *61*, 562−569.
(85) Panov, A. V.; Prokushkin, A. S.; Korets, M. A.; Bryukhanov, A. V.; Myers-Pigg, A. N.; Louchouarn, P.; Sidenko, N. V.; Amon, R.; Andreae, M. O.; Heimann, M. Linking trace gas measurements and molecular tracers of organic matter in aerosols for identification of ecosystem sources and types of wildfires in Central Siberia. In *9th International Multidisciplinary Conference and Early Career Scientists School on Environmental Observations, Modelling and Information Systems (ENVIROMIS)*, Tomsk, RUSSIA, July 11−16, 2016; Tomsk, Russia, 2016.
(86) Fu, P. Q.; Kawamura, K.; Miura, K. Molecular characterization of marine organic aerosols collected during a round-the-world cruise. *J. Geophys. Res.* **2011**, *116*, D13302.
(87) Hu, Q. H.; Xie, Z. Q.; Wang, X. M.; Kang, H.; Zhang, P. F. Levoglucosan indicates high levels of biomass burning aerosols over oceans from the Arctic to Antarctic. *Sci. Rep.* **2013**, *3*, 3119.
(88) Shen, R. Q.; Ding, X.; He, Q. F.; Cong, Z. Y.; Yu, Q. Q.; Wang, X. M. Seasonal variation of secondary organic aerosol tracers in Central Tibetan Plateau. *Atmos. Chem. Phys.* **2015**, *15* (15), 8781−8793.
(89) Reisen, F.; Meyer, C. P.; Keywood, M. D. Impact of biomass burning sources on seasonal aerosol air quality. *Atmos. Environ.* **2013**, *67*, 437−447.
(90) Kleinman, L. I.; Springston, S. R.; Daum, P. H.; Lee, Y. N.; Nunnermacker, L. J.; Senum, G. I.; Wang, J.; Weinstein-Lloyd, J.; Alexander, M. L.; Hubbe, J.; Ortega, J.; Canagaratna, M. R.; Jayne, J. The time evolution of aerosol composition over the Mexico City plateau. *Atmos. Chem. Phys.* **2008**, *8* (6), 1559−1575.
(91) Barten, J. G. M.; Ganzeveld, L. N.; Visser, A. J.; Jimenez, R.; Krol, M. C. Evaluation of nitrogen oxides (NOx) sources and sinks and ozone production in Colombia and surrounding areas. *Atmos. Chem. Phys.* **2020**, *20* (15), 9441−9458.
(92) Hudman, R. C.; Jacob, D. J.; Turquety, S.; Leibensperger, E. M.; Murray, L. T.; Wu, S.; Gilliland, A. B.; Avery, M.; Bertram, T. H.; Brune, W.; Cohen, R. C.; Dibb, J. E.; Flocke, F. M.; Fried, A.; Holloway, J.; Neuman, J. A.; Orville, R.; Perring, A.; Ren, X.; Sachse, G. W.; Singh, H. B.; Swanson, A.; Wooldridge, P. J. Surface and lightning sources of nitrogen oxides over the United States: Magnitudes, chemical evolution, and outflow. *Journal of Geophysical Research-Atmospheres* **2007**, *112* (D12), D12S05.
(93) Verma, S. K.; Kawamura, K.; Chen, J.; Fu, P. Q.; Zhu, C. M. Thirteen years of observations on biomass burning organic tracers over Chichijima Island in the western North Pacific: An outflow region of Asian aerosols. *Journal of Geophysical Research-Atmospheres* **2015**, *120* (9), 4155−4168.
(94) Boreddy, S. K. R.; Kawamura, K. A 12-year observation of water-soluble ions in TSP aerosols collected at a remote marine location in the western North Pacific: an outflow region of Asian dust. *Atmos. Chem. Phys.* **2015**, *15* (11), 6437−6453.
(95) Chen, J.; Kawamura, K.; Liu, C.-Q.; Fu, P. Long-term observations of saccharides in remote marine aerosols from the western North Pacific: A comparison between 1990−1993 and 2006−2009 periods. *Atmos. Environ.* **2013**, *67*, 448−458.
(96) Chen, J. M.; Li, C. L.; Ristovski, Z.; Milic, A.; Gu, Y. T.; Islam, M. S.; Wang, S. X.; Hao, J. M.; Zhang, H. F.; He, C. R.; Guo, H.; Fu,

https://doi.org/10.1021/acs.est.0c07313
Environ. Sci. Technol. XXXX, XXX, XXX−XXX

H. B.; Miljevic, B.; Morawska, L.; Thai, P.; Fat, L.; Pereira, G.; Ding, A. J.; Huang, X.; Dumka, U. C. A review of biomass burning: Emissions and impacts on air quality, health and climate in China. *Sci. Total Environ.* **2017**, *579*, 1000−1034.
(97) Zhang, Y. X.; Shao, M.; Zhang, Y. H.; Zeng, L. M.; He, L. Y.; Zhu, B.; Wei, Y. J.; Zhu, X. L. Source profiles of particulate organic matters emitted from cereal straw burnings. *J. Environ. Sci.* **2007**, *19* (2), 167−175.

https://doi.org/10.1021/acs.est.0c07313
Environ. Sci. Technol. XXXX, XXX, XXX−XXX